Temperature-sensitive Yeast Mutants Defective in Mitochondrial Inheritance

Stephen J. McConnell, Leslie C. Stewart, Alec Talin, and Michael P. Yaffe

University of California, San Diego, Department of Biology, La Jolla, California 92093

Abstract. The distribution of mitochondria to daughter cells is an essential feature of mitotic cell growth, yet the molecular mechanisms facilitating this mitochondrial inheritance are unknown. We have isolated mutants of *Saccharomyces cerevisiae* that are temperature-sensitive for the transfer of mitochondria into a growing bud. Two of these mutants contain single, recessive, nuclear mutations, *mdm1* and *mdm2*, that cause temperature-sensitive growth and aberrant mitochondrial distribution at the nonpermissive temperature. The absence of mitochondria from the buds of mutant cells was confirmed by indirect immunofluorescence microscopy and by transmission electron microscopy. The *mdm1* lesion also retards nuclear division and prevents the transfer of nuclei into the buds. Cells containing the *mdm2* mutation grown at the nonpermissive temperature sequentially form multiple buds, each receiving a nucleus but no mitochondria. Neither *mdm1* or *mdm2* affects the transfer of vacuolar material into the buds or causes apparent changes in the tubulin- or actin-based cytoskeletons. The *mdm1* and *mdm2* mutations are cell-cycle specific, displaying an execution point in late G1 or early S phase.

MITOCHONDRIA proliferate by the growth and division of preexisting mitochondria (Attardi and Schatz, 1988). A consequence of this mode of organelle propagation is that each daughter cell must receive an adequate allotment of mitochondria before the completion of cell division. The mechanisms and cellular structures that mediate this organellar inheritance are unknown.

Studies with cells from a number of diverse organisms have implicated the cytoskeleton as playing a major role in the positioning and distribution of mitochondria. Mitochondria exhibit saltatory motion (Adams, 1982; Aufderheide, 1977) and occupy specific intracellular positions that have been correlated with microtubules in some cell types (Ball and Singer, 1982) and with intermediate filaments in other types of cells (Hirokawa, 1982). Electron microscopy of rapidly frozen frog neurons revealed short cross-bridges of thin filaments connecting mitochondria and microtubules (Hirokawa, 1982). Studies with neuronal cells have documented transport along microtubules as a key component of the axonal transport of mitochondria and other organelles (Vale, 1987), and movement of organelles along microtubules has been described for some nonneuronal cells (Vale, 1987). Elegant reconstitution studies using permeabilized cells or isolated cellular components have identified the proteins kinesin and cytoplasmic dynein as microtubule-based motors involved in the movement of particles along microtubules (Vale, 1987; Schroer et al., 1989), although little is known of the role of these proteins in organellar distribution during mitosis.

The role of microtubules in the distribution of organelles during mitosis (like that of the associated kinesin and dynein) is obscure, since cytoplasmic microtubules largely disassemble at this stage in the cell cycle (Saxton et al., 1984). Studies in the filamentous fungus *Aspergillus nidulans* demonstrated that inhibition of microtubule function with the agent benomyl or by mutations affecting β-tubulin blocked movement and division of the nucleus but had no effect on movement of mitochondria (Oakley and Reinhart, 1985). Additionally, mitochondria and other organelles migrate into the growing buds of yeast cells even in the presence of inhibitors or mutations that disrupt microtubule function (Huffaker et al., 1988; Jacobs et al., 1988).

Actin microfilaments may also play a role in organellar distribution. In some mammalian cells, regions with mitochondrial and organellar streaming movement correlate with areas of change in the structure of actin-like microfilament bundles (Wang and Goldman, 1978). Actin-mediated organellar transport has been characterized in characean algal cells (Kachar and Reese, 1988) where endoplasmic reticulum and other organelles contact actin filament bundles during cytoplasmic streaming. Using an in vitro reconstituted system Adams and Pollard (1986) demonstrated the function of myosin-I in the active translocation of organelles from *Acanthamoeba* along actin microfilaments. Mutations in the single actin gene in *Saccharomyces cerevisiae* interfere with bud formation (Novick and Botstein, 1985), so it is difficult to assess the specific role of actin in mitochondrial movement in these mutants.

One of the earliest events in the cell division cycle of the yeast *Saccharomyces cerevisiae* is the movement of mito-

chondria into the growing bud (Stevens, 1981). Almost as soon as a bud is apparent, a portion of a mitochondrion is found in this region of the cell. As the bud grows it is filled with more mitochondria (and other organelles) until, at cytokinesis, the daughter cell is provisioned with a mitochondrial content slightly exceeding that of the mother cell (Stevens, 1981). This pattern of movement of mitochondria into yeast buds occurs without regard to the carbon source or environmental conditions (e.g., even in cells growing anaerobically on glucose) and appears to be independent of microtubule function (Huffaker et al., 1988) and nuclear division (Thomas and Botstein, 1986). The molecular details and control of this mitochondrial movement have yet to be described.

We have initiated a genetic approach to study the inheritance of mitochondria and identify its molecular basis. We have isolated a number of temperature-sensitive mutants in the yeast *Saccharomyces cerevisiae* which have conditional defects in the transport of mitochondria into a growing bud. Below we describe the isolation of these mutants and the properties of two of the mutant strains.

Materials and Methods

Strains and Genetic Methods

The *mdm* mutants were isolated from a collection of 1,200 temperature-sensitive lethal mutants derived from strain A364A (*MATa adel ade2 ural his7 lys2 tyrl gall*) and obtained from C. McLaughlin (University of California, Irvine, CA). Genetic analysis was as described by Sherman et al. (1979).

Isolation of mdm Mutants

Mutants defective in mitochondrial distribution were isolated by screening a collection of temperature-sensitive strains by microscopic analysis. The screening procedure involved first growing minicultures of the different strains in 0.2 ml of YPG medium (1% bacto-yeast extract, 2% bacto-peptone, 3% glycerol), at 23°C overnight. The cells were then diluted with 0.6 ml of fresh YPG and shifted to the nonpermissive temperature (37°C) for 4 h. 5 μl of cell suspension were mixed with 5 μl of a solution of 50 μg/ml 2-(4-dimethylaminostyryl)-1-methylpyridinium iodide (DASPMI, purchased from Sigma Chemical Co., St. Louis, MO) in water directly on microscope slides, and the cells were observed immediately with the fluorescence microscope using the fluorescein filter set.

Immunofluorescence Microscopy

Cells were fixed and processed for immunofluorescence as described by Kilmartin and Adams (1984) with the modifications described below. Cells were fixed with formaldehyde for 30 min at 37°C, followed by an additional 30 min at 23°C. Cells were not fixed in methanol or acetone. After applying the cells to polylysine-coated multiwell slides, the fixed cells were washed four times with a solution of 2 mg/ml bovine serum albumin in 0.15 M NaCl, 0.05 M potassium phosphate, pH 7.4 (BSA-PBS). Mitochondria were detected using a mouse monoclonal antibody against a 14-kD polypeptide of the yeast mitochondrial outer membrane (OM14) described previously by Riezman et al. (1983). Microtubules were visualized with a rat monoclonal antitubulin antibody (Accurate Chemical and Scientific Corp., Westbury, NY). After incubation of the fixed cells for 2 h with the primary antibodies, the slides were washed eight times with BSA-PBS. Secondary antibodies included rhodamine-conjugated goat anti-mouse IgG for detection of mitochondria and FITC-conjugated goat anti-rat IgG for tubulin detection (both obtained from Jackson Immunoresearch Laboratories, Inc. [West Grove, PA] and diluted 1:40 in BSA-PBS before use). Samples were incubated with the secondary antibody for 2 h, after which the cells were washed eight times with BSA-PBS. DAPI (Sigma Chemical Co.) was added to the samples to 0.1 μg/ml, and slides incubated at room temperature for 5 min. After washing the wells eight additional times with BSA-PBS, the slides were air dried, mounted as described by Kilmartin and Adams (1984), and viewed on a Leitz Laborlux 12 microscope equipped for epifluorescence. Both phase-contrast and fluorescence images were viewed with a Leitz Fluotar 100× PL 1.3 objective under oil immersion. The fluorochromes FITC, rhodamine, and DAPI were viewed using the Leitz selective filter sets L/3, N/2, and A, respectively. Photomicrographs were made using Kodak Tri-X pan, ISO 400 film.

Electron Microscopy

Cells were prepared for electron microscopy as described by Stevens (1977) with the following modifications: Washes with a 0.9% solution of NaCl were done at 37°C, and cells were stained with 2% uranyl acetate solution overnight at 4°C with constant agitation.

Vacuolar Staining

Vacuoles were visualized using the dyes pyranine or quinacrine or by detecting an endogenous fluorescent compound that accumulates in vacuoles of yeast containing the *ade1* or *ade2* mutations (Weisman et al., 1987). Pyranine staining was performed as described by Pringle et al. (1989). For quinacrine staining, cells were first synchronized in G1 phase with α-factor (as described below), shifted to 37°C for 4 h, pelleted in a microcentrifuge, and resuspended in YPD (1% bacto-yeast extract, 2% bacto-peptone, 2% glucose) containing 10 μM quinacrine, 50 mM NaH_2PO_4, pH 7.6. The cells were shaken at 37°C for 4.5 min, pelleted, resuspended in 1 ml fresh YPD, and observed in the fluorescence microscope. To detect vacuoles with the fluorophore accumulated as a result of the *ade* mutations, cells were grown to stationary phase in YPD at room temperature. After back diluting into YPD plus adenine (160 μg/ml), the cells were shifted to 37°C for 4 h and immediately viewed in the fluorescence microscope.

α-Factor, Hydroxyurea, and Nocodazole Treatments

Cell cycle arrest with the yeast mating pheromone α-factor were performed by growing *MATa* cells to 1–2 × 10^7 cells/ml in YPD medium that had been adjusted to pH 4.0 with HCl and sterilized by filtration. α-factor (Sigma Chemical Co.) was added from a 0.5 mg/ml stock solution in ethanol to a concentration of 4 μg/ml, and cells were shaken at room temperature for 4 h. To remove the block to cell cycle progression cells were washed three times with 1 ml YPD (normal pH) and the cell concentration was adjusted to 1 × 10^6 cells/ml in YPD. For hydroxyurea or nocodazole arrests cells were grown to 1 × 10^6 cells/ml in YPD. Hydroxyurea or nocodazole (5 mg/ml stock solution in DMSO; Sigma Chemical Co.) were added to final concentrations of 0.1 M or 12.5 μg/ml, respectively. Cells were incubated with inhibitor for 4 h at 23°C, and inhibition was relieved as described above for α-factor.

Results

Isolation of mdm Mutants

Yeast cells defective in the transmission of mitochondria during mitotic growth were isolated by screening a collection of temperature-sensitive strains for cells that failed to transport mitochondria into developing buds during incubation at the nonpermissive temperature, 37°C. Mitochondria were detected by fluorescence microscopy after staining cells with the mitochondria-specific dye DASPMI (Bereiter-Hahn, 1976). Fig. 1 shows mutant and wild-type cells analyzed with this procedure. 27 strains displaying aberrant mitochondrial distribution were identified from a collection of ~1,000 temperature-sensitive strains. The mutants were backcrossed to a wild-type parental strain, and the haploid progeny from nine of these crosses displayed both temperature-sensitive growth and a failure to segregate mitochondria to buds at 37°C. Complementation analysis indicated that the nine mutant strains belong to eight complementation groups, and we have designated the mutations in these strains *mdm* (mitochondrial distribution and morphology). Below we describe the properties of mutant cells from two complementation groups, *mdm1* and *mdm2* (of which two alleles were isolated, *mdm2-1* and *mdm2-2*).

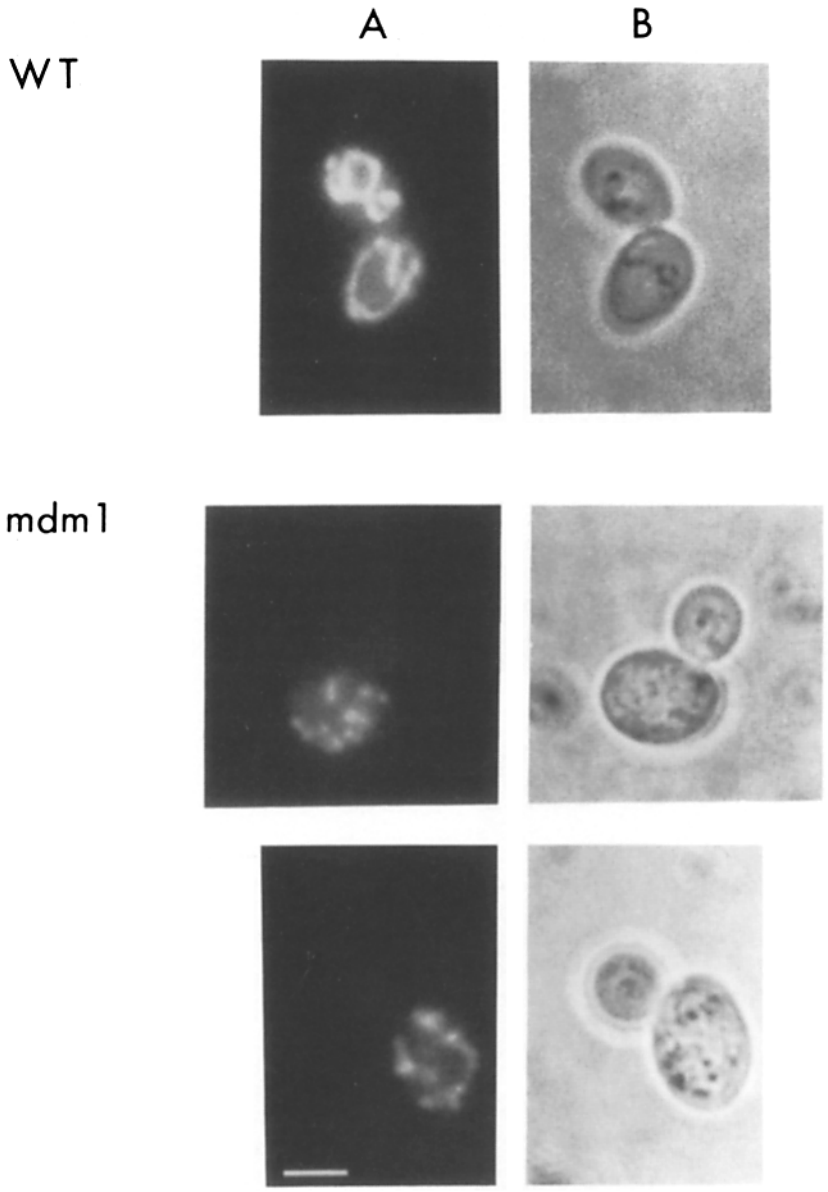

Figure 1. Identification of *mdm* mutants by vital staining of mitochondria. Wild-type and mutant cells were grown overnight at 23°C, diluted with fresh media, and incubated at 37°C for 4 h. Aliquots were removed, mixed with the mitochondria-specific dye DASPMI, and the cells observed by fluorescent illumination and phase-contrast microscopy. Bar, 2 μm.

mdm1 and mdm2 Are Single, Recessive, Nuclear Mutations

To characterize the genetic lesions in *mdm1* and *mdm2* cells, the mutant strains were backcrossed to the wild-type parental strain and the phenotypes of meiotic progeny from the crosses were examined. The temperature-sensitive growth and mitochondrial distribution phenotypes demonstrated 2:2 segregation and complete cosegregation in 30 tetrads derived from *mdm1/MDM1* diploid cells. The same pattern of inheritance was observed for 25 tetrads derived from *mdm2/MDM2* diploids. Diploid cells, heterozygous for either *mdm1* or *mdm2* displayed normal growth and mitochondrial distribution indicating the recessive character of the mutations.

The possibility that two tightly linked mutations were separately responsible for the temperature-sensitive growth and mitochondrial distribution defects (a situation that might not be detected by tetrad analysis) was examined by determining the reversion frequency of the *mdm1* and *mdm2* mutations and analyzing temperature-sensitive growth and mitochondrial distribution in spontaneous revertants. Revertants of *mdm1* and *mdm2* were isolated at frequencies of $\sim 3 \times 10^{-7}$ and 1×10^{-8}, respectively. 20 separately isolated revertants of *mdm1* were analyzed and all were found to have both normal growth and normal mitochondrial distribution at 37°C. Similar observations were made for three revertants of *mdm2*-2. Analysis of the progeny from a cross of the revertant strains to wild-type parents demonstrated that the absence of mutant phenotypes in the revertants was not due to the appearance of secondary, unlinked suppressor mutations. These results, together with those of tetrad analysis, demonstrate that the *mdm1* and *mdm2* mutants carry single, recessive, nuclear mutations.

Mitochondrial Delivery to the Bud Is Defective in mdm1 and mdm2 Cells

The *mdm* mutant cells were identified by the absence of mi-

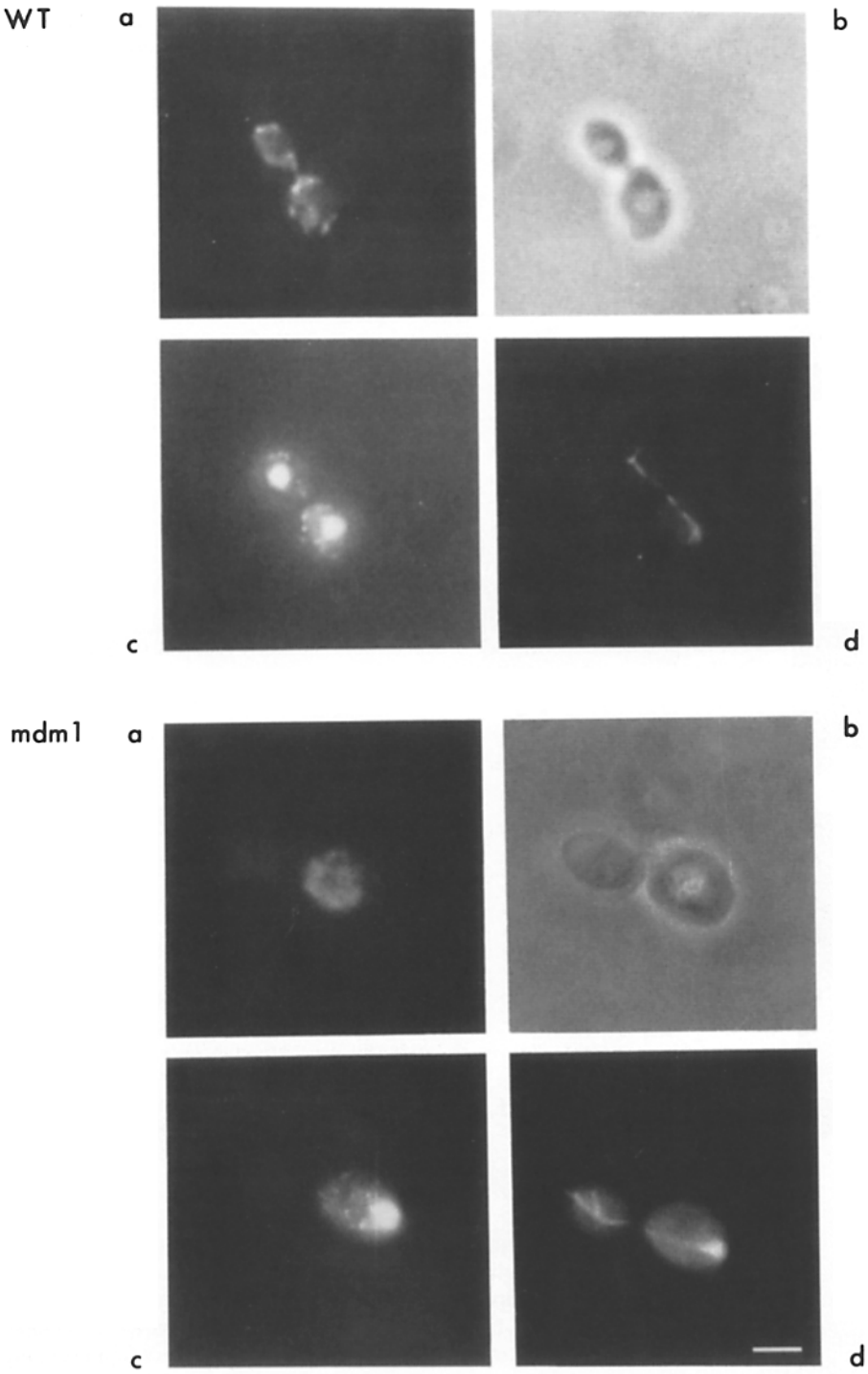

Figure 2. Mitochondria and nuclei are not transported into the buds of *mdm1* cells during incubation at 37°C. Wild-type and *mdm1* mutant cells were grown overnight at 23°C, diluted with fresh media, and incubated at 37°C for 4 h. Cells were then fixed with formaldehyde and processed for indirect immunofluorescence as described in Materials and Methods. Mitochondria (*a*) were visualized using a mouse monoclonal antibody against a yeast mitochondrial outer membrane protein, OM14, followed by rhodamine-conjugated goat anti-mouse IgG as secondary antibody. Nuclei and mitochondrial DNA (*c*) were detected by DAPI staining. Microtubules (*d*) were visualized using a rat monoclonal antitubulin antibody followed by FITC-conjugated goat anti-rat IgG. *b* represents corresponding bright-field images of whole cells. Bar, 2 μm.

tochondrial staining in buds using the mitochondria-specific dye DASPMI. To demonstrate that this lack of bud staining reflected the absence of mitochondria rather than aberrant dye uptake or a localized defect in mitochondrial function in the bud, the mitochondrial distribution in the mutant cells was examined by indirect immunofluorescence microscopy on formaldehyde-fixed cells using an antibody against OM14, a major 14-kD protein of the mitochondrial outer membrane (Riezman et al., 1983). With this analysis, mitochondria were found to be absent from the buds of *mdm1* and *mdm2* cells after incubation for 4 h at the nonpermissive temperature (Fig. 2, *mdm1*, *a*; Fig. 3 *a*). When *mdm1* or *mdm2* cells were first synchronized in the G1 (unbudded) stage with mating pheromone, 100% of the buds that formed during a subsequent incubation at the nonpermissive temperature were devoid of mitochondria. Staining of cellular DNA with DAPI provided a further confirmation of aberrant mitochondrial distribution: the punctate cytoplasmic staining characteristic of mitochondrial DNA is absent from the mutant buds (Fig. 2, *mdm1*, *c*; Fig. 3 *c*). Additionally, the lack of mitochondria in the buds of mutant cells was confirmed by transmission electron microscopy (Fig. 4). The defective delivery of mito-

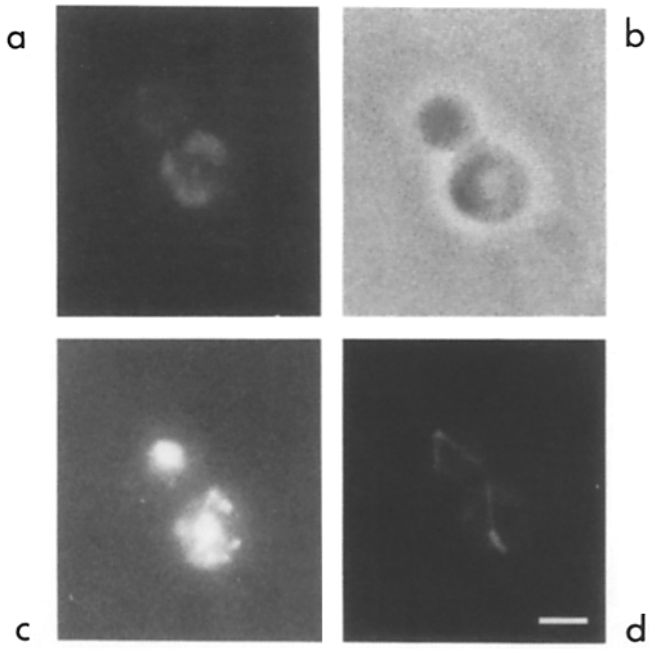

Figure 3. mdm2 cells form buds lacking mitochondria but containing nuclei during incubation at 37°C. Cells containing the *mdm2-1* mutation were grown overnight at 23°C, diluted with fresh media, and incubated at 37°C for 5.5 h. Cells were fixed and analyzed by fluorescence, indirect immunofluorescence, and bright-field microscopy as described for Fig. 2. (*a*) Mitochondria; (*b*) bright field of cell; (*c*) DAPI staining of nuclei and mitochondrial DNA; (*d*) microtubules. Bar, 2 μm.

chondria into the buds of *mdm1* and *mdm2* cells at the nonpermissive temperature was found for cells grown on both respiratory (glycerol) and fermentable (glucose) carbon sources. At the permissive temperature (23°C) mitochondrial distribution in the *mdm1* and *mdm2* cells appeared virtually identical with that found in wild-type cells (data not shown).

In addition to the effects on mitochondrial distribution the *mdm1* and *mdm2* mutations appear to affect the morphology of mitochondria in cells incubated at the nonpermissive temperature. In wild-type cells grown on glucose the mitochondria appear as long snakelike structures (Fig. 1 and see Stevens, 1981), while in *mdm1* cells the mitochondria are more fragmented and beadlike (Fig. 1). Mitochondria in *mdm2* cells grown on glucose appear similar to those in the *mdm1* mutant after incubation at the nonpermissive temperature (data not shown). The mitochondria in *mdm1* and *mdm2* mutant cells grown on glycerol appear slightly smaller but more numerous than those in wild-type cells after incubation at 37°C (Fig. 4).

Nuclei Are Absent from the Buds of mdm1 Cells

DAPI staining of *mdm1* cells that had been shifted to the nonpermissive temperature for 4 h revealed that the *mdm1* lesion also affected nuclear division and resulted in buds devoid of nuclei (Fig. 2 *c*). The nuclei were located within the mother region of the cell and did not move into the neck between the mother and bud. In a small fraction of *mdm1* cells incubated at 37°C for a number of hours, nuclear division did occur, yet both nuclei remained in the mother portion of the cell (Fig. 5). This observation suggests that the *mdm1* mutation also affects the transfer of nuclei into growing buds and/or the orientation of the mitotic spindle with respect to the cellular budding axis.

mdm2 Cells Form Multiple Buds Lacking Mitochondria but Containing Nuclei

Buds formed by *mdm2* cells during incubation at the nonpermissive temperature contained nuclei (Fig. 3 *c*), indicating that this mutation does not affect nuclear division or transmission. Cells containing the *mdm2-2* mutation formed multiple buds, each containing a nucleus but lacking mitochondria (Figs. 6 and 7) during incubation at the nonpermissive temperature. Examination of such cells at various times after a shift to 37°C revealed that the multiple buds were produced sequentially and that the production of each bud was accompanied by a separate round of nuclear division. After synchronization of cells in the unbudded stage, virtually 100% of the new buds that emerged at 37°C were devoid of mitochondria. Second buds began appearing ~2 h after a shift of a culture to 37°C. By 5 h after a temperature shift, doubly budded cells were very abundant in the population, and cells with three buds began appearing. *mdm2-1* cells also formed multiple buds, but the second buds developed only after very long incubations at the nonpermissive temperature (data not shown).

Effects of the mdm1 and mdm2 Mutations on the Tubulin and Actin Cytoskeletons

The tubulin cytoskeleton was characterized in *mdm1* and *mdm2* cells by indirect immunofluorescence microscopy. Most *mdm1* cells incubated for several hours at the nonpermissive temperature contained a long cytoplasmic microtubule extending into the bud (Fig. 2 *d*). Although of longer length, this microtubule appeared qualitatively similar to the cytoplasmic microtubule found extended into the buds in wild-type cells early in the cell cycle (Adams and Pringle, 1984; Kilmartin and Adams, 1984). Additionally, in *mdm1* cells incubated for long periods at 37°C, a thickening of the microtubule associated with the nucleus in the mother portion of the cell was observed (not shown). This thickening suggested spindle pole body duplication (Kilmartin and Adams, 1984). In *mdm1* cells in which nuclear division had occurred (as discussed above), the mitotic spindle appeared similar to those seen in wild-type cells but was entirely contained within the mother portion of the cell. Additionally, a cytoplasmic-type microtubule often extended from one end of the spindle into the bud (data not shown). Furthermore, the presence of two nuclei in these cells indicated the proper functioning of microtubules in chromosomal separation and nuclear division.

The microtubules in *mdm2* cells incubated at the nonpermissive temperature were very similar to those found in wild-type cells (Fig. 2, *wt, d*; Fig. 3 *d*; Fig. 6 *d*). Additionally, the multiple rounds of nuclear division, which give rise to the nuclei in each bud of the multiply budded *mdm2* cells (as described above), suggested normal microtubule function in chromosome separation, nuclear migration, and nuclear division.

The actin distribution in *mdm1* and *mdm2* cells (data not shown) resembled that found in the wild-type cells (Adams and Pringle, 1984; Kilmartin and Adams, 1984). In cells

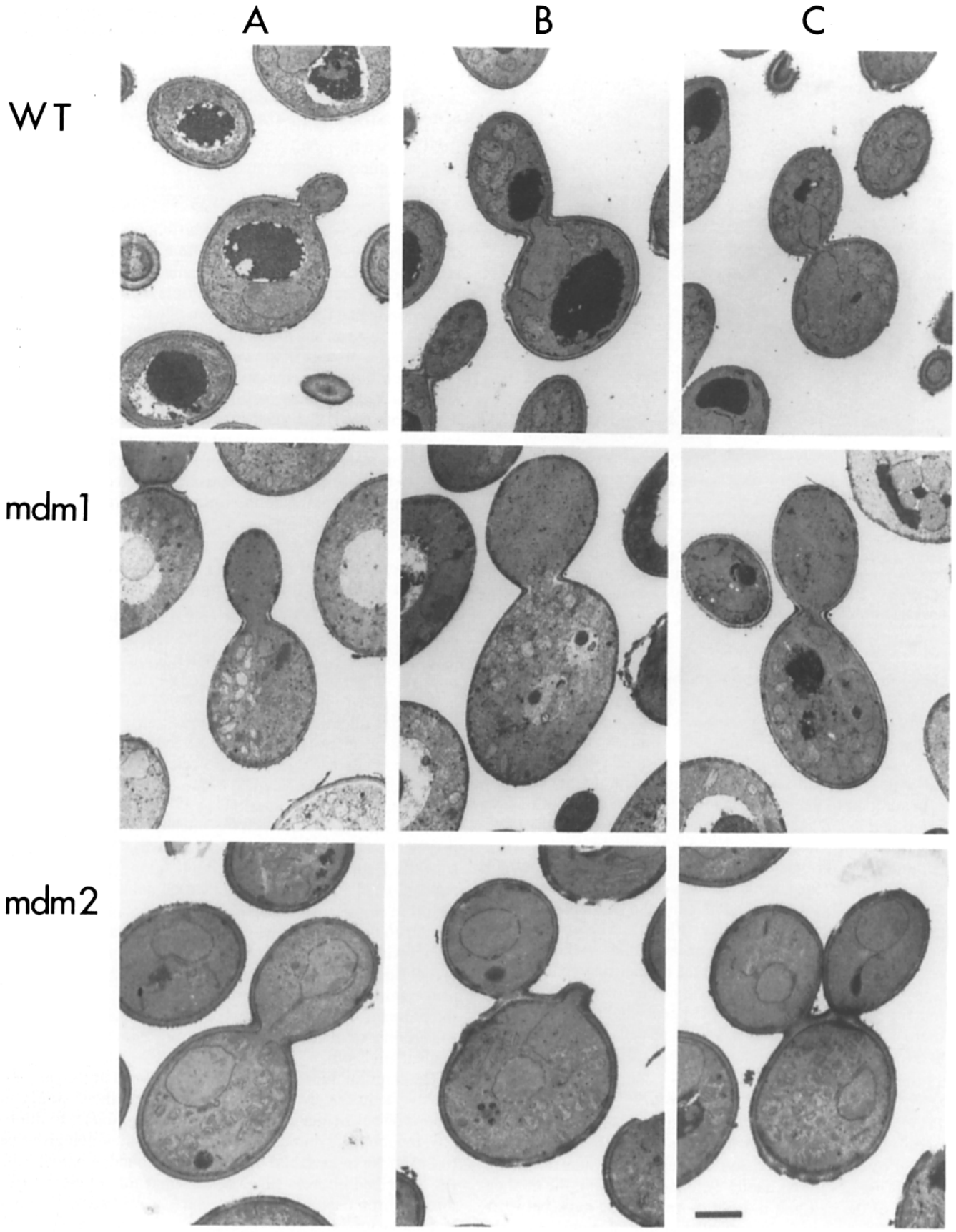

Figure 4. Transmission electron microscopy of *mdm* mutant cells. Cells were grown in YPG to a final OD_{600} of 0.5 and shifted to 37°C for 4 h for *mdm1* cells and 5.5 h for wild-type and *mdm2* cells. Cells were prefixed in glutaraldehyde, fixed in $KMnO_4$, and stained in uranyl acetate overnight. Sections were stained subsequently with lead citrate. Shown are three different cells of each type. Bar, 1 μm.

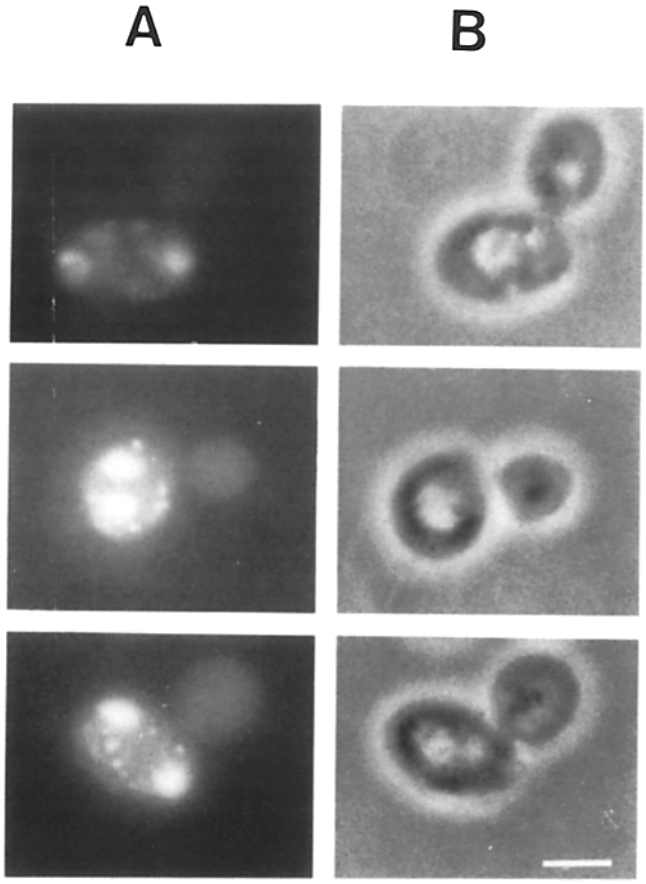

Figure 5. Nuclei in *mdm1* cells do not migrate into the bud even when complete nuclear division occurs. *mdm1* cells were shifted to the nonpermissive temperature for 4 h, fixed with formaldehyde, and stained with DAPI as described in Materials and Methods. Three different cells viewed with fluorescence and bright-field microscopy are shown. Bar, 2 μm.

with small buds, actin was found concentrated in the bud, with actin fibers running into the mother portion of the cell. Cells with larger buds contained actin arranged in a series of cortical spots located throughout the cell. These patterns were detected at both permissive and nonpermissive temperatures in the mutant cells. Thus, the *mdm1* and *mdm2* mutations do not appear to have direct or dramatic effects on the tubulin and actin cytoskeletons.

Vacuoles Are Transferred to Buds in mdm1 and mdm2 Cells

Studies by Weisman et al. (1987) have indicated that buds acquire vacuoles quite early in the cell cycle and that the bud's vacuolar contents are largely inherited from the vacuoles in the mother portion of the cell. To examine the effects of the *mdm1* and *mdm2* mutations on vacuolar distribution and inheritance, vacuoles were examined microscopically after the incubation of mutant cells at the nonpermissive temperature. Both fluorescence microscopic analysis of cells treated with vacuole-specific vital dyes and analysis by transmission electron microscopy demonstrated the presence of vacuoles in buds formed at the nonpermissive temperature in *mdm1* and *mdm2* cells (data not shown). Furthermore, fluorescent vacuolar material that had accumulated in pre-existing vacuoles (in the mother portion of the cell) as a result of an *ade2* mutation was transferred to vacuoles in newly formed buds of *mdm1* cells during incubation at 37°C (Fig. 8). A similar transfer of fluorescent vacuolar material was observed with *mdm2* cells (data not shown). These experiments indicate that the *mdm1* and *mdm2* mutations do not affect the segregation and inheritance of vacuoles.

mdm1 and mdm2 Defects Are Cell-Cycle Specific

Cultures of *mdm1* and *mdm2* cells shifted to 37°C for a number of hours contained many cells with large (empty) buds, suggesting an effect of the mutations on the cell cycle. Neither *mdm1* nor *mdm2* cells arrested as a morphologically homogeneous population after long incubation at the nonpermissive temperature indicating that they are not classical *cdc* mutants (Pringle and Hartwell, 1981). Additionally, an analysis of a large number of previously isolated *cdc* mutants failed to reveal any defects in mitochondrial distribution in these strains (McConnell, S. J., and M. P. Yaffe, unpublished observations). However, to eliminate the possibility that the *mdm* mutants might represent new alleles of previously identified *cdc* mutants, complementation tests were performed between cells carrying the *mdm1* or *mdm2* mutations and a number of *cdc* mutants which arrest with large single or multiple buds. Complementation of the temperature-sensitive phenotypes was found in every instance (data not shown) indicating that *mdm1* and *mdm2* are unique from the known *cdc* mutants.

To further characterize the relationship between the *mdm* mutations and cell-cycle progression, mutant cells were first synchronized at several points in the cell cycle, and then their progress through the cycle was examined after a shift to the nonpermissive temperature. Mutant *mdm1* or *mdm2* yeast synchronized as unbudded, G1 cells with the mating pheromone α-factor formed small empty buds which grew progressively into large empty buds (data not shown). In contrast, *mdm1* and *mdm2* cells synchronized in S phase or in mitosis completed the initial cell cycle after a shift to the nonpermissive temperature, and in the subsequent cycle the cells put out new buds which were deficient of mitochondria (data not shown). These observations indicate that the execution points for the *mdm1* and *mdm2* mutations occur in late G1 or early S phase.

Discussion

Cells containing the *mdm1* or *mdm2* mutations are defective in the transmission of mitochondria to the growing bud during incubation at the nonpermissive temperature. The absence of mitochondria from the buds of these cells was confirmed by indirect immunofluorescence microscopy to detect a major mitochondrial outer membrane protein (Figs. 2, 3, 6, and 7), the absence of DAPI staining characteristic of mitochondrial DNA (Figs. 2, 3, and 5–8), and by electron microscopic analysis (Fig. 4). Periodic observations of cells first synchronized in the G1 (unbudded) phase and then allowed to develop buds during incubation at 37°C revealed that the large empty buds were derived from new buds that had received no mitochondria rather than via the removal or destruction of mitochondria already present in buds.

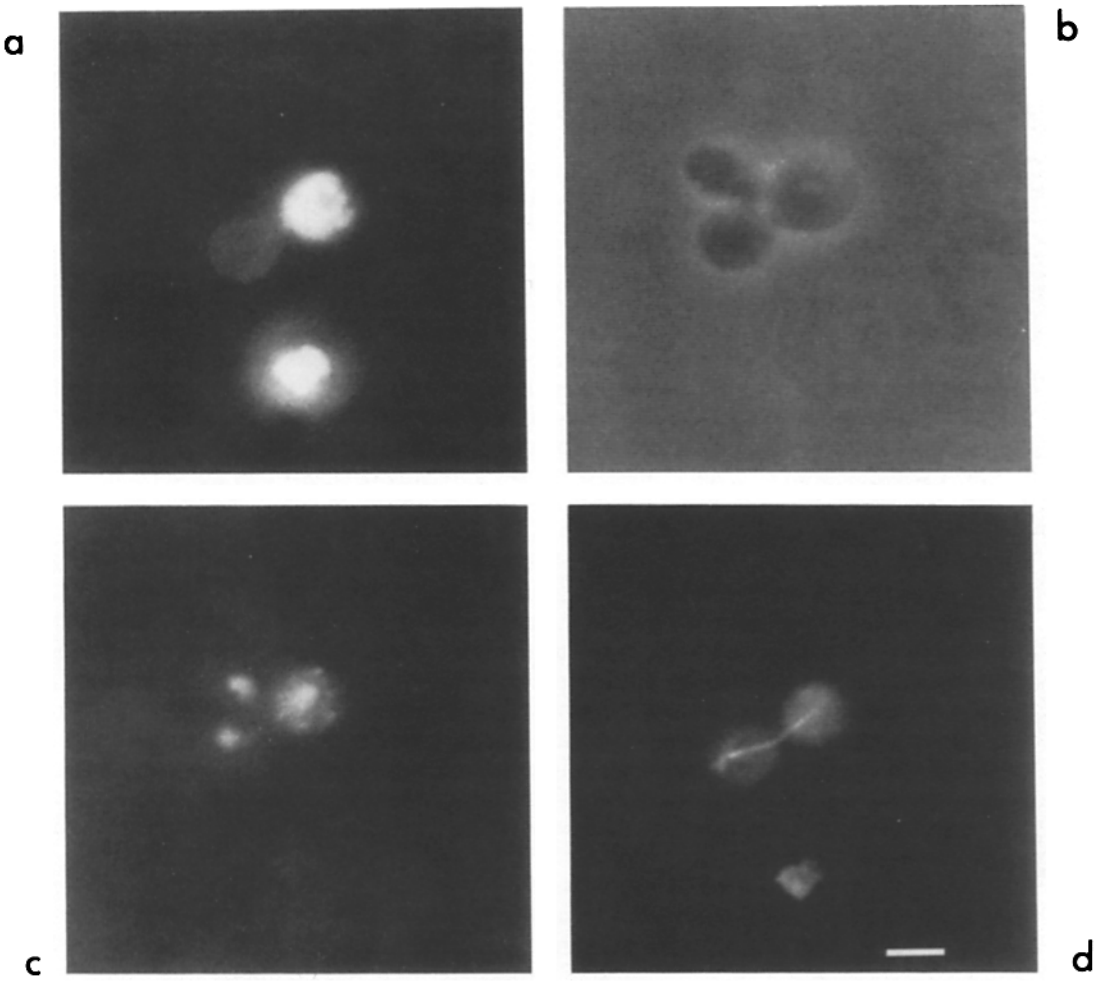

Figure 6. *mdm2-2* cells form multiple buds, each with a nucleus but lacking mitochondria during incubation at 37°C. *mdm2-2* Cells were grown overnight at 23°C, shifted to 37°C for 6 h, fixed with formaldehyde, and processed for indirect immunofluorescence as described in Fig. 2 and Materials and Methods. (*a*) Mitochondrial staining; (*b*) bright-field image of whole cell; (*c*) DAPI staining of nuclei and mitochondrial DNA; (*d*) microtubule staining. Bar, 2 μm.

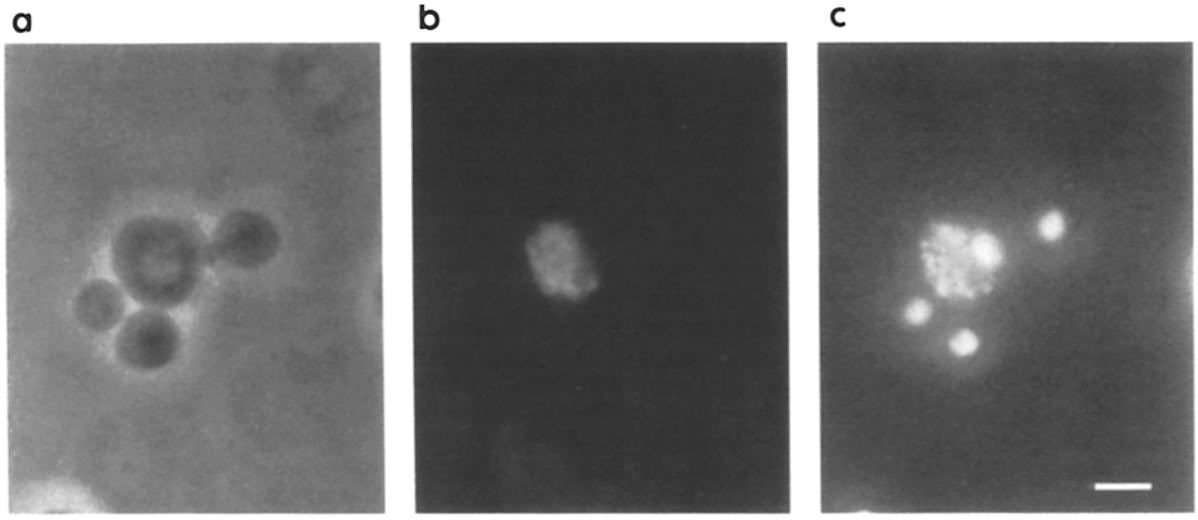

Figure 7. An *mdm2* cell with three buds. *mdm2-2* cells were grown overnight at 23°C, shifted to 37°C for 6 h, and processed for fluorescence and indirect immunofluorescence microscopy as described for Fig. 2. (*a*) Bright field of cell; (*b*) mitochondria; (*c*) DAPI staining of nuclei and mitochondrial DNA. Bar, 2 μm.

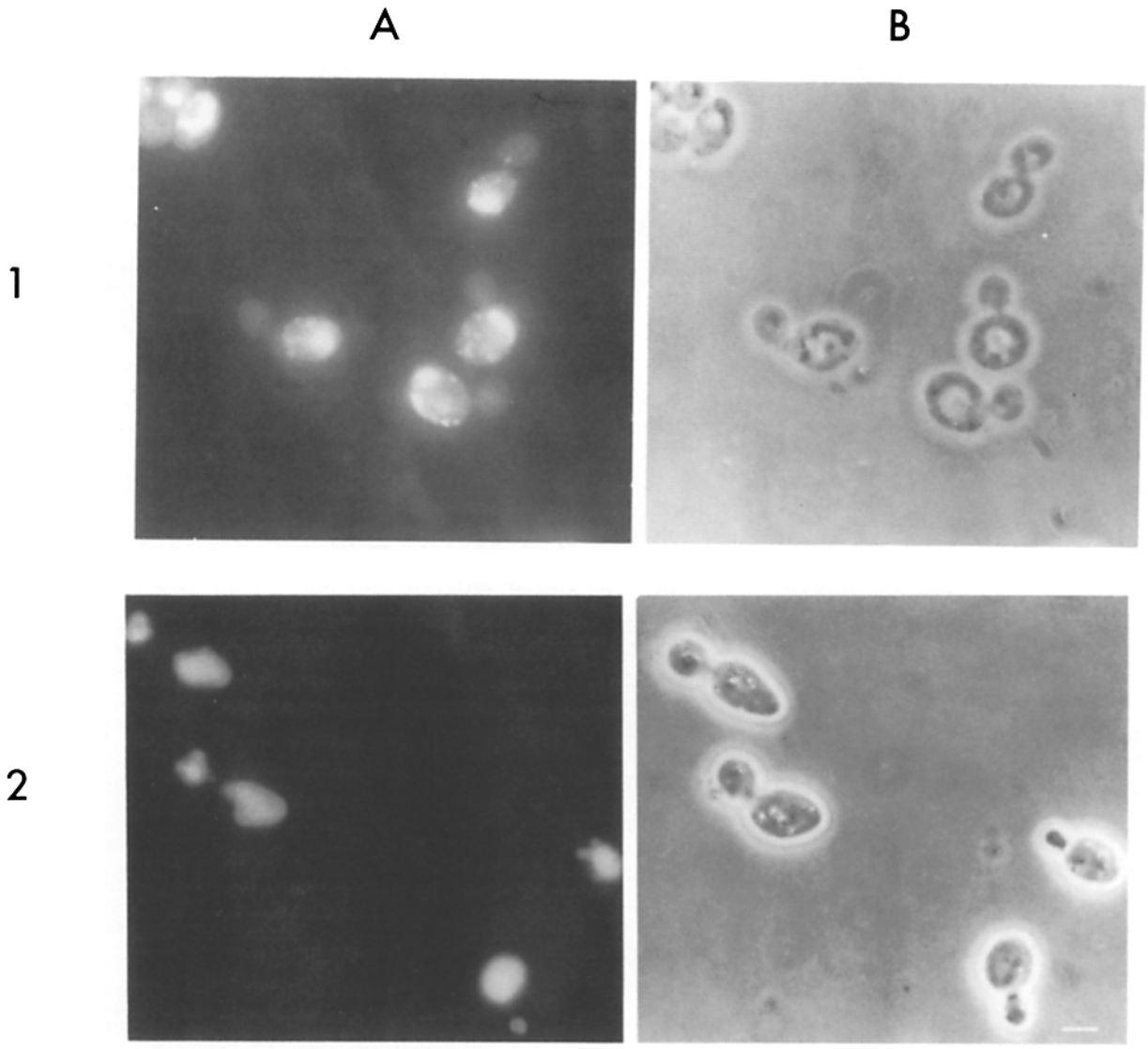

Figure 8. Vacuoles are present in the buds of *mdm1* mutant cells. *mdm1* cells containing the *ade1* and *ade2* mutations were grown to stationary phase in YPD medium until fluorescent vacuolar material was observed. Cells were then diluted into fresh YPD supplemented with adenine (to a concentration of 160 μg/ml), and shifted to 37°C for 4 h. DAPI staining was used to visualize nuclear and mitochondrial DNA (*1 A*), and vacuoles observed directly by fluorescence microscopy (*2 A*). Phase-contrast images of whole cells appear in *1 B* and *2 B*. Bar, 2 μm.

The isolation of mutants defective in mitochondrial inheritance and the characteristics of the mutant cells support the idea that mitochondrial transfer into the bud is an active and specific process. All of the *mdm* mutations analyzed thus far are recessive, consistent with the loss of a function necessary for mitochondrial movement. The possibility that an obstruction caused by the mutation prevents the transfer of mitochondria appears unlikely since no obstacle is evident by electron microscopic analysis (Fig. 4), and other organelles (e.g., vacuoles in both mutants and nuclei in *mdm2* cells) are able to enter the buds. In some mutant cells mitochondria have actually entered the bud but have not been distributed throughout the bud cytoplasm (Fig. 4, *mdm1, b*) further suggesting that the distribution mechanism is defective.

The *mdm1* and *mdm2* mutations also appear to affect the morphology of mitochondria, causing more fragmented and, in some cases, smaller organelles (Figs. 1 and 4). The relationship between these morphological changes and the defects in mitochondrial distribution are unknown. Changes in both mitochondrial distribution and mitochondrial morphology may be primary effects of the genetic lesion or one of the phenotypes might be a secondary consequence of an alteration in the other process. For example, defective mitochondrial division secondarily might prevent transfer of the organelles into the bud. However, we have detected no evidence of defective mitochondrial proliferation or division in the mutant cells. Additionally, the changes in mitochondrial morphology at the nonpermissive temperature do not appear to affect mitochondrial function in energy metabolism, as mutant cells still develop and enlarge buds during incubation at 37°C on glycerol, a nonfermentable (mitochondria-requiring) carbon source. Also, the mitochondria in mutant cells incubated for many hours at the nonpermissive temperature still take up the fluorescent DASPMI dye, an uptake

dependent on the mitochondrial membrane potential (Bereiter-Hahn, 1976).

Although the cytoskeleton has been implicated in the movement and positioning of mitochondria in a number of previous studies (Adams, 1982; Ball and Singer, 1982; Hirokawa, 1982; Vale, 1987; Wang and Goldman, 1978), the aberrant mitochondrial transport in *mdm1* and *mdm2* cells does not appear to result from defects in the tubulin or actin-based cytoskeletons. First, microtubules extend into the buds of both *mdm1* and *mdm2* cells (Figs. 2 and 3). Second, nuclear division, a process dependent on microtubule function, occurs normally in *mdm2* cells and takes place in a fraction of *mdm1* cells at the nonpermissive temperature (Fig. 5). Third, actin distribution appears normal in *mdm1* and *mdm2* cells (data not shown), and no defect is apparent in bud formation and growth, a process that depends on actin function (Novick and Botstein, 1985). Cells containing *mdm1* or *mdm2* mutations may be defective in some other cytoskeletal component or in actin- or tubulin-associated proteins.

The *mdm1* mutation affects the transport of both mitochondria and nuclei into the bud. This mutation also appears to retard or inhibit nuclear division in most cells (Fig. 3). Nuclear division does occur at the nonpermissive temperature in a small but significant fraction of *mdm1* cells. In these cells both nuclei are restricted to the mother portion of the cell (Fig. 5), indicating a lack of nuclear migration into the mother-bud neck and a disorientation of the mitotic spindle from its normal alignment with the axis of budding. While cytoplasmic microtubules have been implicated in nuclear migration and spindle positioning in yeast (Huffaker et al., 1988), the structures with which these microtubules interact and which orient the mitotic spindle along the axis of budding are unknown. These structures may also play a role in mitochondrial movement and may be defective in the *mdm1* mutant.

The *mdm2* mutation appears specific for the transfer of mitochondria into the developing bud. Nuclei, vacuoles, and other subcellular structures are found in buds of *mdm2* cells after incubation at 37°C (Figs. 3 and 4). The mutant cells go through successive, multiple rounds of bud formation and nuclear division, yet fail to form independent, viable progeny even on media that can sustain nonrespiratory growth. This observation is consistent with previous studies (Kovacova et al., 1968; Gbelska et al., 1983; Yaffe and Schatz, 1984) that suggested that mitochondria supply some essential cellular functions in addition to their role in energy metabolism.

The properties of the *mdm1* and *mdm2* mutants demonstrate that events of mitochondrial inheritance can be separated from bud development, nuclear division, and vacuolar segregation, and imply that mitochondrial distribution is a specific and active process. The mutants will be valuable tools for the further study of mitochondrial inheritance. The genes defined by these mutants will be isolated and analyzed to identify their protein products. The study of these proteins in mutant and wild-type cells should facilitate an understanding of the molecular basis of this essential process.

We gratefully acknowledge the assistance of Lance Washington with the electron microscopy and Michelle Apperson for backcrossing of mutant strains. We thank Lois Weisman for her advice on visualizing vacuoles. We are grateful to Jon Singer and Bill Loomis for critical reading of the manuscript.

This work was supported by a Searle Scholarship (to M. P. Yaffe) from the Searle Scholars Program of the Chicago Community Trust.

Received for publication 5 March 1990 and in revised form 2 May 1990.

References

Adams, A. E. M., and J. R. Pringle. 1984. Relationship of actin and tubulin distribution to bud growth in wild-type and morphogenetic-mutant *Saccharomyces cerevisiae*. *J. Cell Biol.* 98:934–945.

Adams, R. J. 1982. Organelle movement in axons depends on ATP. *Nature (Lond.)*. 297:327–329.

Adams, R. J., and T. D. Pollard. 1986. Propulsion of organelles isolated from *Acanthamoeba* along actin filaments by myosin-I. *Nature (Lond.)*. 322: 754–756.

Attardi, G., and G. Schatz. 1988. Biogenesis of mitochondria. *Annu. Rev. Cell Biol.* 4:289–333.

Aufderheide, K. J. 1977. Saltatory motility of uninserted trichocysts and mitochondria in *Paramecium tetraurelia*. *Science (Wash. DC)*. 198:299–300.

Ball, E. H., and S. J. Singer. 1982. Mitochondria are associated with microtubules and not with intermediate filaments in cultured fibroblasts. *Proc. Natl. Acad. Sci. USA*. 79:123–126.

Bereiter-Hahn, J. 1976. Dimethylaminostyrylmethylpyridiniumiodide (DASPMI) as a fluorescent probe for mitochondria in situ. *Biochim. Biophys. Acta*. 423:1–14.

Gbelska, Y., J. Subik, A. Goffeau, and L. Kovac. 1983. Intramitochondrial ATP and cell functions: yeast cells depleted of intramitochondrial ATP lose the ability to grow and multiply. *Eur. J. Biochem.* 130:281–286.

Hirokawa, N. 1982. Cross-linker system between neurofilaments, microtubules, and membranous organelles in frog axons revealed by the quick-freeze, deep-etching method. *J. Cell Biol.* 94:129–142.

Huffaker, T. C., J. H. Thomas, and D. Botstein. 1988. Diverse effects of β-tubulin mutations on microtubule formation and function. *J. Cell Biol.* 106:1997–2010.

Jacobs, C. W., A. E. M. Adams, P. J. Szaniszlo, and J. R. Pringle. 1988. Functions of microtubules in the *Saccharomyces cerevisiae* cell cycle. *J. Cell Biol.* 107:1409–1426.

Kachar, B., and T. S. Reese. 1988. The mechanism of cytoplasmic streaming in *Characean* algal cells: sliding of endoplasmic reticulum along actin filaments. *J. Cell Biol.* 106:1545–1552.

Kilmartin, J. V., and A. E. M. Adams. 1984. Structural rearrangements of tubulin and actin during the cell cycle of the yeast *Saccharomyces*. *J. Cell Biol.* 98:922–933.

Kovacova, V., J. Irmlerova, and L. Kovac. 1968. Oxidative phosphorylation in yeast. IV. Combination of a nuclear mutation affecting oxidative phosphorylation with a cytoplasmic mutation to respiratory deficiency. *Biochim. Biophys. Acta*. 162:157–163.

Novick, P., and D. Botstein. 1985. Phenotypic analysis of temperature-sensitive yeast actin mutants. *Cell*. 40:405–416.

Oakley, B. R., and J. E. Reinhart. 1985. Mitochondria and nuclei move by different mechanisms in *Aspergillus nidulans*. *J. Cell Biol.* 101:2392–2397.

Pringle, J. R., and L. H. Hartwell. 1981. The *Saccharomyces cerevisiae* cell cycle. *In* The Molecular Biology of the Yeast *Saccharomyces cerevisiae*. Vol. 1. J. N. Strathern, E. W. Jones, and J. R. Broach, editors. Cold Spring Harbor Laboratory, Cold Spring Harbor, NY. 97–142.

Pringle, J. R., R. A. Preston, A. E. M. Adams, T. Stearns, D. G. Drubin, B. K. Haarer, and E. W. Jones. 1989. Fluorescence microscopy methods for yeast. *Methods Cell Biol.* 31:357–435.

Riezman, H., R. Hay, S. Gasser, G. Daum, G. Schneider, C. Witte, and G. Schatz. 1983. The outer membrane of yeast mitochondria: isolation of outside-out sealed vesicles. *EMBO (Eur. Mol. Biol. Organ.) J.* 2:1105–1111.

Saxton, W. M., D. L. Stemple, R. J. Leslie, E. D. Salmon, M. Zavortink, and J. R. McIntosh. 1984. Tubulin dynamics in cultured mammalian cells. *J. Cell Biol.* 99:2175–2186.

Schroer, T. A., E. R. Steuer, and M. P. Sheetz. 1989. Cytoplasmic dynein is a minus end-directed motor for membranous organelles. *Cell*. 56:937–946.

Sherman, F., G. R. Fink, and J. B. Hicks. 1979. Methods in Yeast Genetics. Cold Spring Harbor Laboratory, Cold Spring Harbor, NY. 98 pp.

Stevens, B. 1981. Mitochondrial structure. *In* The Molecular Biology of the Yeast *Saccharomyces cerevisiae*. Vol. 1. J. N. Strathern, E. W. Jones, and J. R. Broach, editors. Cold Spring Harbor Laboratory, Cold Spring Harbor, NY. 471–504.

Stevens, B. J. 1977. Variation in number and volume of the mitochondria in yeast according to growth conditions. A study based on serial sectioning and computer graphics reconstruction. *Biol. Cell*. 28:37–56.

Thomas, J. H., and D. Botstein. 1986. A gene required for the separation of chromosomes on the spindle apparatus in yeast. *Cell*. 44:65–76.

Vale, R. D. 1987. Intracellular transport using microtubule-based motors. *Annu. Rev. Cell Biol.* 3:347–378.

Wang, E., and R. D. Goldman. 1978. Functions of cytoplasmic fibers in intracellular movements in BHK-21 cells. *J. Cell Biol.* 79:708–726.

Weisman, L. S., R. Bacallao, and W. Wickner. 1987. Multiple methods of visualizing the yeast vacuole permit the evaluation of its morphology and inheritance through the cell cycle. *J. Cell Biol.* 105:1539–1547.

Yaffe, M. P., and G. Schatz. 1984. Two nuclear mutations that block mitochondrial protein import in yeast. *Proc. Natl. Acad. Sci. USA*. 81:4819–4823.